1 Early Universe Physics

1.1 Chronology of the Early Universe

t	$T \propto \rho^{1/4}$	Redshift	Event
10^{-43} s	10^{19} GeV	∞	Planck energy, Quantum gravity? Big Bang Singularity?
10^{-38} s	10^{16} GeV	∞	Inflation ends? Grand Unification Scale? Baryogenesis?
10^{-11} s	100 GeV	10^{15}	Electroweak phase transition (spontaneous symmetry breaking)
10^{-5} s	150 MeV	10^{12}	Quark-hadron (QCD) phase transition ($T_c \simeq \Lambda_{\rm QCD}$)
1 sec	1 MeV	6×10^9	ν_e decoupling ($\nu_e \approx 1$ MeV, $\nu_\mu, \nu_\tau \approx 3$ MeV)
6 sec	500 keV	2×10^9	$e\bar{e}$ annihilation
3 min	100 keV	4×10^8	Nucleosynthesis (BBN)
60 kyr	0.75 eV	3200	Matter-radiation equality
300 kyr	0.3 eV	1100	Atom formation, photon decoupling (CMB)
400 Myr	5 meV	~ 10	Reionization
9 Gyr	0.33 meV	0.4	Dark energy-matter equality
Now	10^{-4} eV (2.73 K)	0	now

At the early Universe, the Universe was denser and hotter, dominated by the relativistic particles and radiation. Because of its high energy, particles and anti-particle pairs are created and annihilated. This process depends on the particle contents of our nature. The standard model of particle physics is well tested and understood up to ~ 1 TeV (horizontal line in the table), beyond which the predictions from the standard model are somewhat uncertain and other beyond-the-standard-model physics have vastly different predictions. Our discussion will be limited to the standard model physics.

In this radiation dominated era, almost all particles behave like massless particles, and their energy density evolves as radiation $\rho \propto 1/a^4$. In RDE, the Hubble expansion and the age of the Universe are well approximated in terms of the equilibrium temperature T of the plasma as

$$H \simeq 0.3\ \text{sec}^{-1} \sqrt{g_*} \left(\frac{T}{1\ \text{MeV}}\right)^2 , \qquad t = \frac{1}{2H} \simeq 1\ \text{sec} \left(\frac{T}{1\ \text{MeV}}\right)^{-2} g_*^{-1/2} , \tag{1.1}$$

where g_* is the total spin-degeneracy factor shown in Figure 1.1. Particles stay in thermal equilibrium with the plasma, as long as their interaction rate Γ with the plasma remains sufficiently high:

$$\Gamma = n \langle \sigma v \rangle \geq H , \tag{1.2}$$

where σ is the interaction cross section $[\sigma] = L^2$, v is the relative velocity of the particles in interaction, and n is the particle number density. Note that the interaction rate is averaged over the particle velocity distribution. A useful conversion relation is

$$1\ \text{MeV} = 1.602 \times 10^{-6}\ \text{erg} = 1.161 \times 10^{10}\ \text{K} . \tag{1.3}$$

At $T < 10^{16}$ GeV, the dominant interaction among the relativistic particles is mediated by massless gauge bosons, and the cross section is $\sigma \sim \alpha^2/T^2$, such that the interaction rate is $\Gamma \propto n\sigma v \sim \alpha^2 T$, where the $SU(2)$ gauge coupling constant is $g = 1/\sqrt{4\pi\alpha}$ and we used $n \propto T^3$, $v \sim 1$. Therefore, the interaction is efficient to maintain the thermal equilibrium

$$\frac{\Gamma}{H} \sim \frac{10^{16}\text{GeV}}{T} \gg 1 \quad \text{for } T < 10^{16}\ \text{GeV} . \tag{1.4}$$

At lower temperature $T < 300$ GeV, the interactions are now mediated by *massive* gauge bosons (e.g., $m_Z \simeq 100$ GeV), and the cross section is $\sigma \sim G_F^2 T^2$, such that the interaction rate is $\Gamma \propto G_F^2 T^5$. Therefore, the interaction is again efficient to maintain the thermal equilibrium up to $T > 1$ MeV,

$$\frac{\Gamma}{H} \sim G_F^2 T^3 \sim \left(\frac{T}{1\ \text{MeV}}\right)^3 \gg 1 \quad \text{for } T > 1\ \text{MeV} , \tag{1.5}$$

where the Fermi constant is $G_F = 1.15 \times 10^{-5}$ GeV^{-2}. Then, the question arises: what happens at $T > 10^{16}$ GeV? The Universe might not have been in thermal equilibrium at such early time.

A brief overview of the most important cosmological events are as follows (Mo et al., 2010):

- At $T \gg 1$ TeV, two important events must take place: inflationary expansion and baryogensis. An inflationary expansion for a very short period of time must have taken place to explain some of the key problems in observational cosmology, and some mechanism beyond the standard model must have been in operation to generate the asymmetry between baryons and anti-baryons we observe today. The former is highly constrained and relatively well understood, while the latter is very poorly understood. Beyond these two events that must have happened in the early Universe, there might have been other interesting events in other beyond-the-standard-model physics such as the grand unification. During this stage, quarks and gluons are not bound to hardronic states, such that there exist no protons, neutrons and so on. The Universe was made of fundamental elementary particles, forming a hot plasma (or soup).
- At $T \sim$150 MeV ($t \sim 10^{-5}$ sec), the quark–hadron phase transition occurs, confining quarks into hadrons, and the chiral symmetry is broken. Lattice QCD calculations show that the electroweak and QCD phase transitions are smooth. Once the transition was complete, the Universe was filled with a hot plasma consisting of three types of relativistic pions $\pi^{\pm}$, π^0 ($m_{\pi^\pm} = 139.6$ MeV, $m_{\pi^0} = 135.0$ MeV), non-relativistic nucleons (p, n), relativistic leptons $e^{\pm}$, $\mu^{\pm}$ ($m_\mu = 105$ MeV), and their associated neutrinos ($\nu_e, \bar{\nu}_e, \nu_\mu, \bar{\nu}_\mu, \nu_\tau, \bar{\nu}_\tau$), and photons, all in thermal equilibrium. Heavier lepton τ ($m_\tau = 1.78$ GeV) have already annihilated, and only a trace amount due to lepton asymmetry must have remained.
- At $T \sim 100$ MeV ($t \sim 10^{-4}$ sec), pions become non-relativistic, and $\pi^{\pm}$-pairs annihilate each other, while the neutral pions π^0 decay into photons. From this point on, protons and neutrons are the only hadronic species left. At about the same time, muons $\mu^{\pm}$ start to annihilate.
- At $T \sim 1$ MeV ($t \sim 1$ sec), electrons and positrons become non-relativistic, annihilating each other. At about the same time, e-neutrinos ν_e also decouple from the hot plasma. μ- and τ-neutrinos decouple a bit earlier than e-neutrinos. The weak interactions become ineffective, and the ratio of neutrons to protons is frozen.
- At $T \sim 0.1$ MeV ($t \sim 3$ minutes), the Big Bang Nucleosynthesis (BBN) starts, synthesizing protons and neutrons to produce D, He and a few other heavy elements. This nuclear fusion is exactly the same as one at the core of stars, but it takes place everywhere in the Universe.
- At $T \sim 4000$ K ($t \sim 2 \times 10^5$ yr), free electrons and protons recombine to form neutral hydrogen atoms. The Universe then becomes transparent to photons, and these free-streaming photons are observed today as the cosmic microwave background (CMB) in a black-body distribution.
- dark age, first stars, cosmic reionization, habitable planets and life formation, dark energy domination

1.2 Thermal Equilibrium in the Early Universe

1.2.1 Chemical Potential

• ***Thermodynamic Quantities***.— Consider creating a system with internal energy U in an environment with temperature T. The Helmholtz free energy $F = U - TS$ is needed to create such system with the help from the environment, where S is the entropy of the final system. In a given environment, the system tends to minimize the internal energy or maximize the entropy, i.e., minimize the Helmholtz free energy. At the minimum of the Helmholtz free energy, the system reaches the thermal equilibrium. The Enthalpy $H = U + PV$ is similar, but such system is created from a small volume, that more energy for PV work is needed. Finally, the Gibbs free energy is the combination of all: $G = U - TS + PV$. They are all related by the Legendre transformation.

• ***Legendre Transformation***.— converts a function of a set of variables to another function of their conjugate variables. For example, consider a function $f(x, y)$. The conjugate variables of (x, y) are (U, W)

$$U := \left(\frac{\partial f}{\partial x}\right)_y , \qquad W := \left(\frac{\partial f}{\partial y}\right)_x , \qquad df = U\, dx + W\, dy\, . \tag{1.6}$$

Table 1.1: Particles in the Standard Model

particle	mass	g_i
γ	0	2
$\nu,\ \bar{\nu}$	≈ 0	6
$e^+,\ e^-$	0.51 MeV	4
$\mu^+,\ \mu^-$	106 MeV	4
$\pi^+,\ \pi^-$	135 MeV	2
π^0	140 MeV	1
$gluons$	0	16
$u,\ \bar{u}$	5 MeV	12
$d,\ \bar{d}$	9 MeV	12
$s,\ \bar{s}$	115 MeV	12
$c,\ \bar{c}$	1.3 GeV	12
$\tau^+,\ \tau^-$	1.8 GeV	4
$b,\ \bar{b}$	4.4 GeV	12
$W^+,\ W^-$	80 GeV	6
Z	91 GeV	3
H	114 GeV	1
$t,\ \bar{t}$	174 GeV	12

Now consider a combination of two variables Wy and a new function $g := f - Wy$:

$$d(Wy) = y\,dW + W\,dy\,, \qquad dg = df - d(Wy) = U\,dx - y\,dW\,, \tag{1.7}$$

which implies that the function g has two independent variables x and W:

$$g = g(x, W)\,, \qquad U = \left(\frac{\partial g}{\partial x}\right)_W\,, \qquad y = -\left(\frac{\partial g}{\partial W}\right)_x\,. \tag{1.8}$$

In this way, three functions can be obtained by Legendre transforming $f(x, y)$ with two variables.

• ***Chemical Potential***.— Consider a thermodynamic system, in which particles are created and annihilated. The amount of energy needed to create a particular species is called the chemical potential (by definition):

$$dU =: TdS - PdV + \sum_{i=1}^{n} \mu_i dN_i\,, \qquad \mu_i = \left(\frac{\partial U}{\partial N_i}\right)_{S,V,N_{j\neq i}}\,, \tag{1.9}$$

when the entropy and the volume of the system are held fixed. While exact in the definition, it is in practice difficult to find a situation, where the volume and the entropy is held fixed. Instead, the other relation is more illuminating for the meaning of the chemical potential:

$$dG = -SdT + VdP + \sum_{i=1}^{n} \mu_i dN_i\,, \qquad \mu_i = \left(\frac{\partial G}{\partial N_i}\right)_{T,P,N_{j\neq i}}\,. \tag{1.10}$$

In thermodynamic equilibrium with constant temperature and pressure, the system exchange particles with its environments. Then we have

$$dG = 0\,, \qquad \sum_{i=1}^{n} \mu_i dN_i = 0\,. \tag{1.11}$$

The chemical potential μ is independent of its fundamental physical properties of particles, but determined by the interactions and the thermodynamic system (e.g., what is conserved). However, since photons are always created and absorbed by a black body, its chemical potential is always zero in equilibrium. Another example is the electron pair production process:

$$\mathrm{env} + \gamma + \gamma \longleftrightarrow e + \bar{e} + \mathrm{env}\,, \qquad 2\,\mu_\gamma = \mu_e + \mu_{\bar{e}}\,, \qquad \therefore\ \mu_e = -\mu_{\bar{e}}\,, \tag{1.12}$$

in which the chemical potential of a particle and its anti-particle has the opposite sign.

1.2.2 Equilibrium Distribution

As long as the scattering process or the interactions between particles are rapid, particles are in kinetic equilibrium, and their phase-space distribution function $f(x,p,t)$ is described by the thermal equilibrium distribution:

$$f(p,t)d^3\mathbf{p} = \frac{g}{(2\pi)^3}\frac{d^3\mathbf{p}}{\exp[(E-\mu)/T]\pm 1}\,, \qquad \begin{cases} + & : \text{Fermion} \\ - & : \text{Boson} \end{cases}\,, \tag{1.13}$$

where g is the spin-degeneracy factor for a given phase-space density and $(2\pi\hbar)^3$ is the unit phase-space volume. Mind that our convention assumes $\hbar = c = k = 1$. In a homogeneous and isotropic background universe, the position dependence and directional dependence vanish. The physical quantities of such particle distribution are

$$n(t) = \int d^3\mathbf{p}\, f(p,t) = \frac{g}{2\pi^2}\int_m^\infty \frac{\sqrt{E^2-m^2}\,EdE}{\exp[(E-\mu)/T]\pm 1}\,, \tag{1.14}$$

$$\rho(t) = \int d^3\mathbf{p}\, Ef(p,t) = \frac{g}{2\pi^2}\int_m^\infty \frac{\sqrt{E^2-m^2}\,E^2dE}{\exp[(E-\mu)/T]\pm 1}\,, \tag{1.15}$$

$$P(t) = \int d^3\mathbf{p}\,\frac{1}{3}\frac{p^2}{E}f(p,t) = \frac{g}{6\pi^2}\int_m^\infty \frac{(E^2-m^2)^{3/2}\,dE}{\exp[(E-\mu)/T]\pm 1}\,, \tag{1.16}$$

where the isotropic pressure is derived from $P = \frac{1}{3}n\langle pv\rangle$ and $v = p/E$. Since the baryon to photon number ratio is so small,

$$\eta := \frac{n_b}{n_\gamma} \simeq 5\times 10^{-10}\,, \tag{1.17}$$

the chemical potential of all species may be approximated as zero for computing the thermodynamic quantities of the early Universe, where photons with $\mu_\gamma = 0$ are the dominant. The ratio of the lepton number density to the photon is also expected to be the same as η.

For non-relativistic particles ($m \gg T$, $E \simeq m$), the distinction between Fermionic and Bosonic particles disappear, and they all follow the classical Maxwell-Boltzmann distribution

$$f(p,t) = \frac{g}{(2\pi)^3}\exp\left(-\frac{m-\mu}{T}\right)\exp\left(-\frac{p^2}{2mT}\right)\,. \tag{1.18}$$

By integrating the distribution, we obtain

$$n(t) = g\left(\frac{mT}{2\pi}\right)^{3/2}\exp\left[-\frac{m-\mu}{kT}\right]\,, \qquad \rho(t) = mn\,, \qquad P(t) = nkT \tag{1.19}$$

In contrast, for relativistic particles ($T \gg m$, $T \gg \mu$), the physical quantities are

$$n(t) = \begin{cases} \frac{g}{\pi^2}\zeta(3)\left(\frac{kT}{\hbar c}\right)^3 & : \text{Boson} \\ \frac{3g}{4\pi^2}\zeta(3)\left(\frac{kT}{\hbar c}\right)^3 & : \text{Fermion} \end{cases}\,, \qquad \rho(t) = \begin{cases} \frac{g\pi^2}{30}kT\left(\frac{kT}{\hbar c}\right)^3 & : \text{Boson} \\ \frac{7}{8}\frac{g\pi^2}{30}kT\left(\frac{kT}{\hbar c}\right)^3 & : \text{Fermion} \end{cases}\,, \qquad P(t) = \frac{1}{3}\rho(t) \tag{1.20}$$

where the Riemann-Zeta function is

$$\zeta(n) := \sum_{i=1}^\infty \frac{1}{i^n}\,, \qquad \zeta(3) \simeq 1.202\,. \tag{1.21}$$

Since the number density of non-relativistic particles in thermal equilibrium is exponentially suppressed, only the relativistic components matter in determining the thermodynamic quantities of the system:

$$n_{\rm tot}(T) = \frac{\zeta(3)}{\pi^2}g_{*,n}T^3\,, \qquad \rho_{\rm tot}(T) = \frac{\pi^2}{30}g_*T^4\,, \qquad P_{\rm tot}(T) = \frac{1}{3}\rho(T)\,, \tag{1.22}$$

where we assumed $\mu_i \equiv 0$ for all species and defined

$$g_{*,n} := \sum_{i\in\text{Boson}} g_i\left(\frac{T_i}{T}\right)^3 + \left(\frac{3}{4}\right)\sum_{i\in\text{Ferm.}} g_i\left(\frac{T_i}{T}\right)^3\,, \qquad g_* := \sum_{i\in\text{Boson}} g_i\left(\frac{T_i}{T}\right)^4 + \left(\frac{7}{8}\right)\sum_{i\in\text{Ferm.}} g_i\left(\frac{T_i}{T}\right)^4\,. \tag{1.23}$$

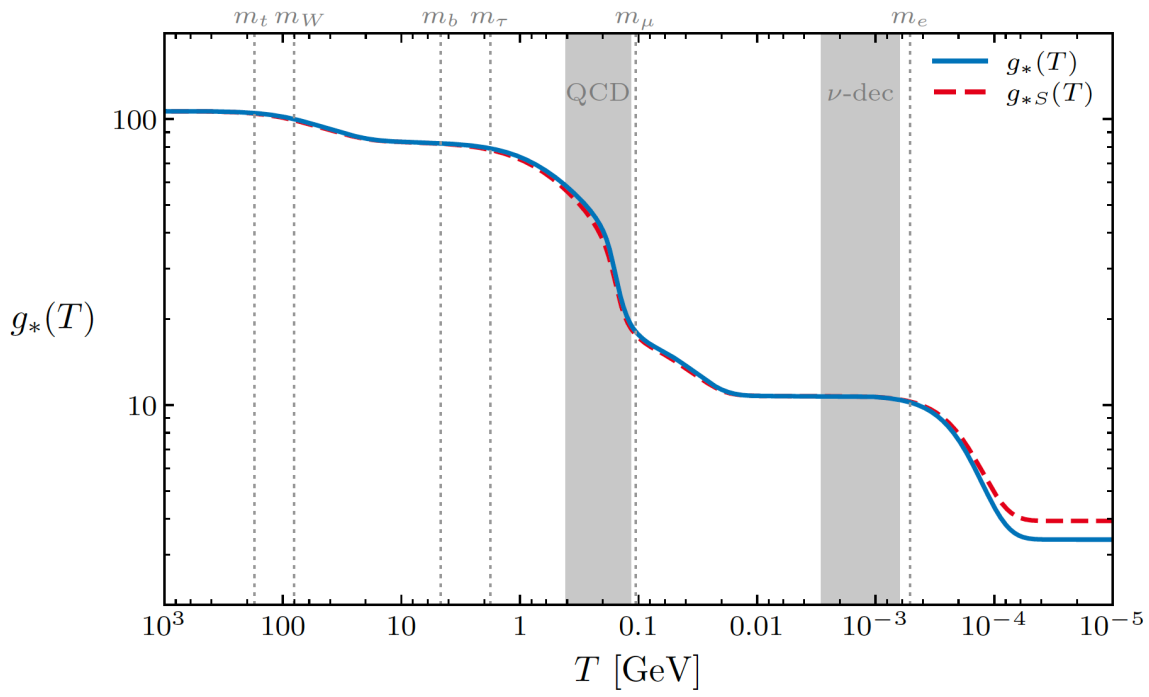

Figure 1.1: Effective number of relativistic dof. The gray bands represent the QCD phase transition and the neutrino decoupling. The difference around 1 TeV is due to the non-perturbative QCD effect. Taken from Baumann et al.

1.2.3 Entropy Density

In the early Universe, particles are created and annihilated. As the Universe expands and cools, some particles annihilate and disappear. Hence the total number is *not* conserved. So, it is useful to have some quantity that is related to the conservation law, i.e., entropy density $s(T)$. Assuming $\mu \equiv 0$, the entropy density for relativistic particles is defined as

$$s := \frac{1}{T}(\rho + P)_{\rm tot} = g_{*,s}\left(\frac{2\pi^2}{45}\right) T^3 \,, \qquad g_{*,s} := \sum_{i\in{\rm Boson}} g_i \left(\frac{T_i}{T}\right)^3 + \left(\frac{7}{8}\right) \sum_{i\in{\rm Ferm.}} g_i \left(\frac{T_i}{T}\right)^3 \,. \tag{1.24}$$

We will show that the conservation of total entropy of the Universe states

$$S := sa^3 \,, \qquad \frac{d}{dt}S = 0 \,, \qquad g_{*,s}^{1/3}(T)\, T \propto \frac{1}{a} \,. \tag{1.25}$$

The thermodynamic laws $TdS = dU + PdV$ apply to the whole system, which is the Universe in our case. The total energy or entropy, etc of the Universe are ill-defined. Instead, we look for local densitites that represent the entropy, i.e., the entropy density s.

Taking the derivative of $P(t)$ with respect to T of a fluid and treating the chemical potential as a function of T, we obtain

$$\frac{dP}{dT} = -\frac{4\pi}{3}\int_0^\infty dp\,(p^3 T)\left(\frac{df}{dp}\right)\left[\frac{E}{T^2} + \frac{d}{dT}\left(\frac{\mu}{T}\right)\right] \,, \qquad \frac{df}{dp} = -\frac{p}{ET}\, f^2(p,t) \exp\left(\frac{E-\mu}{T}\right) \,, \tag{1.26}$$

and with integration by part we re-write the derivative as

$$\frac{dP}{dT} = \frac{\rho + P}{T} + nT\frac{d}{dT}\left(\frac{\mu}{T}\right) \approx \frac{\rho + P}{T} \,. \tag{1.27}$$

Manipulating the conservation equation

$$\dot\rho + 3H(\rho + P) = 0 \,, \qquad d\left(\rho a^3\right) = -P d\left(a^3\right) \,, \qquad \frac{d}{dT}\Big[(\rho + P)a^3\Big] = a^3\frac{dP}{dT} \,, \tag{1.28}$$

we can arrive at the conservation equation

$$d(sa^3) = -\left(\frac{\mu}{T}\right) d(na^3) \approx 0 \,, \qquad\qquad s := \frac{\rho + P}{T} - \frac{n\mu}{T} \approx \frac{\rho + P}{T} \,. \tag{1.29}$$

In most cases, the chemical potential is negligible ($\mu \ll T$) or the number density is conserved ($n \propto 1/a^3$), such that the combination (sa^3) is conserved throughout the evolution. Simplifying the relations for s and dP/dT by assuming $\mu \equiv 0$, we obtain the thermodynamic relation

$$\frac{dT}{T} = \frac{dP}{\rho + P} \,, \qquad\qquad S := sa^3 \,, \qquad\qquad TdS = d\left[(\rho + P)a^3\right] - (\rho + P)a^3 \frac{dT}{T} = d\left(\rho a^3\right) + P\, d(a^3) \,, \tag{1.30}$$

with which we can identify s defined above as the entropy density and the total entropy S is conserved. Hence during the radiation dominated era, the energy density scales as

$$\rho \propto g_* T^4 \propto g_*\, g_{*s}^{-4/3} a^{-4} \,. \tag{1.31}$$

1.2.4 Spin degeneracy factors

The spin degeneracy factor accounts for the number of degenerate states at the same energy level. The photon has two polarization ($g_\gamma = 2$), while neutrinos are only left-handed ($g_\nu = 1$). Note that there exist three generations (ν, μ, τ) of neutrinos and their anti-particles ($\bar\nu$, $\bar\mu$, $\bar\tau$). Spin-1/2 fermions like electrons have $g_e = 2$, and there exist three generations and their anti-particles.

At $T > 300$ GeV, there exist 8 gluons ($g_g = 2$), 3 weak gauge bosons ($W^\pm$, Z), Higgs doublet ($m_H = 125$ GeV), three generations of quarks ($g_q = 2$; two quarks per generation per color) and leptons (g_e, g_ν) to yield[1]

$$g_* = g_\gamma + 8 \times g_g + 3 \times g_{W^\pm,Z} + g_H + \frac{7}{8} \times 3 \times (3 \times 2 \times 2 \times g_q + 2 \times g_\nu + 2 \times g_e) = 106.75 \,. \tag{1.32}$$

At 150 MeV gluons hadronize, and soon after most of the particles become non-relativistic, according to their mass ($m_H = 125$ GeV, $m_Z = 91$ GeV, $m_{W^\pm} = 80$ GeV, $m_\tau = 1.78$ GeV, $m_\mu = 105$ MeV). So at $T \sim 100$ MeV, there left only photons, electrons, and three generations of neutrinos:

$$g_* = g_\gamma + \frac{7}{8}\left(2 \times g_e + 2 \times 3 \times g_\nu\right) = 10.75 \,. \tag{1.33}$$

At a freeze-out temperature $T \sim 1$ MeV, all three generations of neutrinos decouple from the rest of the plasma ($T_\tau \simeq 3.7$ MeV, $T_\mu \simeq 2.4$ MeV, $T_\nu \simeq 1$ MeV), and its temperature strictly declines as $T_\nu \propto 1/a$, since its $g_{*,s}$ remains unchanged, after the decoupling. However, at about $T_\gamma \sim 0.51$ MeV, electrons and anti-electrons become non-relativistic, and they annihilate intro photons , transferring its entropy to the photon plasma, but not to the decoupled neutrinos, which slows the decline of T_γ. Assuming an instantaneous transfer of entropy, the change in the spin-degeneracy factor of the photon plasma can be computed as

$$g_{*,s}^{\rm before} = g_\gamma + \frac{7}{8}\left(g_e + g_{\bar e}\right) = \frac{11}{2} \quad \to \quad g_{*,s}^{\rm after} = g_\gamma \,. \tag{1.34}$$

Given the conservation of $g_{*,s} T^3$ throughout the annihilation, the neutrino temperature is slightly lower than the photon temperature, after the annihilation event

$$T_\nu = \left(\frac{4}{11}\right)^{1/3} T_\gamma \propto \frac{1}{a} \,, \tag{1.35}$$

and the spin degeneracy factor is then

$$g_* = g_\gamma + \frac{7}{8}\left(2 \times 3 \times g_\nu\right) \times \left(\frac{4}{11}\right)^{4/3} = 3.36 \,. \tag{1.36}$$

[1] After the spontaneous symmetry breaking, the weak gauge bosons are massive ($g_{W^\pm,Z} = 3$), and the Higgs boson is left with only one dof ($g_H = 1$), such that there exist 10 dof. Mind that at this energy scales, they are all non-relativistic. However, before the symmetry breaking, the gauge bosons are massless ($g_{W^\pm,Z} = 2$), and the Higgs boson doublet has full dof ($g_H = 4$; two per each component), such that the total dof remains the same.

The total radiation density (γ, ν) is then

$$\rho_{\rm rad} = \left[1 + N_\nu \times \frac{7}{8}\left(\frac{4}{11}\right)^{4/3}\right]\rho_\gamma\,, \qquad N_\nu = 3\,, \qquad \rho_\gamma = a_B T_\gamma^4\,, \tag{1.37}$$

where the radiation constant a_B is related to the Stefan-Boltzmann constant σ_B as

$$a_B = \frac{4\sigma_B}{c} = 7.573\times10^{-15}\,{\rm erg\,cm^{-3}K^{-4}}\,. \tag{1.38}$$

In fact, at the annihilation of electrons and anti-electrons, the neutrino decoupling was incomplete, and some entropy is dumped into neurinos as well. Hence the the neutrino temperature relation above is not precise, and the correction is often rephrased as the effective relativistic degrees of freedom: $N_\nu = 3.04$. The evolution of the spin degeneracy factors is shown in Figure 1.1. Today the photon plasma cools down to

$$T_\gamma = 2.73\,{\rm K}\,, \qquad n_\gamma = 413\,{\rm cm^{-3}}\,, \qquad \rho_\gamma = 4.7{\times}10^{-34}\,g\,{\rm cm^{-3}}\,, \qquad \omega_\gamma = 2.5{\times}10^{-5}\,. \tag{1.39}$$

The cosmic neutrino plasma is

$$T_\nu = 1.95\,{\rm K}\,, \qquad n_{\nu+\bar\nu} = 113\,{\rm cm^{-3}}\,, \qquad n_{\forall\nu} = 338\,{\rm cm^{-3}}\quad(\nu{+}\mu{+}\tau)\,, \qquad \omega_\nu = 1.7{\times}10^{-5}\,, \tag{1.40}$$

for massless neutrinos. Assuming they are relativistic at decoupling, the massive neutrinos

$$\rho_\nu = 113\,m_\nu\,{\rm cm^{-3}}\,, \qquad \omega_\nu = 0.1\left(\frac{m_\nu}{10\,{\rm eV}}\right)\,. \tag{1.41}$$

1.3 Distribution of Decoupled Species

As the Universe expands and cools down, the interaction rate Γ between species falls below the expansion rate $H(t)$, so that a particle species decouples from the plasma. This is called "freeze-out" because there exist no further interactions and its distribution remains frozen. Since the momentum of both massless and massive particles redshifts as $1/a$ in the background universe, the current phase-space distribution of a decoupled species can be expressed in terms of the equilibrium distribution at decoupling:

$$f(p,t) = f_{\rm eq}\left(p\frac{a}{a_{\rm dec}}, t_{\rm dec}\right)\,, \qquad t \geq t_{\rm dec}\,, \qquad p(t_{\rm dec}) = p\frac{a}{a_{\rm dec}}\,. \tag{1.42}$$

When a relativistic species is decoupled at $T_{\rm dec} \gg m$, the Fermi-Dirac or Bose-Einstein distribution is maintained, and hence the number density is as abundant as photons, but the freeze-out condition dictates its temperature declines as $1/a$:

$$f(p,t) = \frac{g}{(2\pi)^3}\left[\exp\left(\frac{p\,a}{a_{\rm dec}T_{\rm dec}}\right) \pm 1\right]^{-1}\,, \qquad T(t) = T_{\rm dec}\frac{a_{\rm dec}}{a}\,, \tag{1.43}$$

where $E \simeq p$ for relativistic particles. Note that the decoupled species evolves separately, so that the change in the spin-degeneracy factor in the other plasma is irrelevant here.

However, when particles are non-relativistic ($T \ll m$) at decoupling, the distribution function is the Maxwell-Boltzmann distribution, and according to the freeze-out condition, the temperature of the decoupled species declines faster than the relativistic particles

$$f(p,t) = \frac{g}{(2\pi)^3}\exp\left(-\frac{m}{T_{\rm dec}}\right)\exp\left(-\frac{p^2a^2}{2m\,a_{\rm dec}^2T_{\rm dec}}\right)\,, \qquad T(t) = T_{\rm dec}\left(\frac{a_{\rm dec}}{a}\right)^2\,, \tag{1.44}$$

where the exponential $\exp(-m/T_{\rm dec})$ is constant. Consequently, the number density of a decoupled species evolves as

$$n(t) = \left[\frac{a(t_{\rm dec})}{a(t)}\right]^3 n_{\rm eq}(t_{\rm dec})\,, \tag{1.45}$$

for both relativistic and non-relativistic particles.

Using the entropy conservation in Eq. (1.25), we obtain the temperature ratio and the number density ratio of a decoupled relativistic species to the photons as

$$\left[\frac{T_\gamma(t_{\rm dec})}{T_\gamma(t)}\right]^3 = \frac{g_{*,s}(t)}{g_{*,s}(t_{\rm dec})}\frac{a^3(t)}{a^3(t_{\rm dec})}\,, \qquad\qquad \frac{n(t)}{n_\gamma(t)} = \frac{g_{\rm eff}}{2}\left[\frac{T(t)}{T_\gamma(t)}\right]^3 = \frac{g_{\rm eff}}{2}\frac{g_{*,s}(T)}{g_{*,s}(T_{\rm dec})}\,, \tag{1.46}$$

where $g_{\rm eff} = g$ for bosons and $g_{\rm eff} = 3g/4$ for fermions and we used the temperature of the decoupled species $T(t_{\rm dec}) = T_\gamma(t_{\rm dec})$ at the time of decoupling.

1.3.1 Boltzmann Equation and Relic Number Density

The particle interactions involve multiple species, and they depend on the velocity distribution of the particles. Consequently, solving for their evolution requires coupled differential equations, called the Boltzmann equation. Consider an interaction $\psi + a + b + \cdots \leftrightarrow i + j + \cdots$ that involves many particles and their creation and annihilation. The Boltzmann equation for a species ψ (similarly for other particles) is

$$\frac{df_\psi}{dt} = C_\psi[f]\,, \tag{1.47}$$

where the right-hand side C is called the collision term that depends on the interaction and the distribution functions of the other particles in interaction. In the absence of collision, the Liouville theorem states that the phase-space distribution is conserved. In a homogeneous and isotropic universe, the phase-space distribution function cannot depend on a position or a direction, i.e., $f_\psi = f_\psi(p,t)$,

$$\frac{df_\psi}{dt} = \frac{\partial f_\psi}{\partial t} + \frac{\partial p}{\partial t}\frac{\partial f_\psi}{\partial p}\,, \qquad\qquad \frac{\partial p}{\partial t} = -Hp\,, \tag{1.48}$$

where we used $p \propto 1/a$ for any particles in the background universe. Integrating over the momentum, we derive that the number density evolves as

$$\frac{dn_\psi}{dt} + 3Hn_\psi = \int d^3p\, C_\psi[f]\,, \qquad\qquad n_\psi = \int d^3p\, f_\psi\,. \tag{1.49}$$

In the absence of collision, the number density decreases as $n_\psi \propto 1/a^3$, and the term $3Hn_\psi$ is called the Hubble drag (or friction) due to the expansion of the Universe.

The collision term depends on the interaction process, and formally it can be expressed as

$$\begin{aligned}\int d^3p\, C_\psi[f] \;=\; & \left(\prod_i \int d^4p_i\right)(2\pi)^4\delta^D(p_\psi + p_a + \cdots - p_i - p_j - \cdots) \\ & \times\left[|\mathcal{M}|^2_{\leftarrow} f_i f_j \cdots (1\pm f_\psi)(1\pm f_a)\cdots - |\mathcal{M}|^2_{\rightarrow} f_a \cdots f_\psi(1\pm f_i)(1\pm f_j)\cdots\right].\end{aligned} \tag{1.50}$$

The first line is just the energy-momentum conservation of the process, the second line shows the interaction of consideration. The invariant matrix element $\mathcal{M}$ can be derived from the QFT calculations, and with T-invariance (or CP-invariance) it is identical in both directions ($|\mathcal{M}|^2 := |\mathcal{M}|^2_{\rightarrow} = |\mathcal{M}|^2_{\leftarrow}$). The distribution functions $f_i f_j \cdots$ in the second line indicates that more particles $i, j, \cdots$ create more particles $\psi, a, b, \cdots$, and vice versa. The extra factors such as $(1 \pm f_\psi)$ are called the Pauli block $(-)$ or the Bose enhancement $(+)$.

For the moment, the collision term is macroscopically treated, and a significant simplification can be made, if most species but ψ are in thermal equilibrium and the temperature is low $T \ll E - \mu$. Consider a simplified interaction $\psi + \bar\psi \leftrightarrow X + \bar X$, in which ψ and $\bar\psi$ annihilate and a pair of X and $\bar X$ are created. At this low temperature $T \ll E - \mu$, the number densities of particles can be written as

$$n = \int d^3p\, f = e^{\mu/T} n_{\rm EQ}\,, \qquad\qquad n_{\rm EQ} := \int d^3p\, f_{\rm EQ}\,, \qquad\qquad f_{\rm EQ} := f(\mu \equiv 0) \simeq \frac{g}{(2\pi)^3} e^{-E/T}\,, \tag{1.51}$$

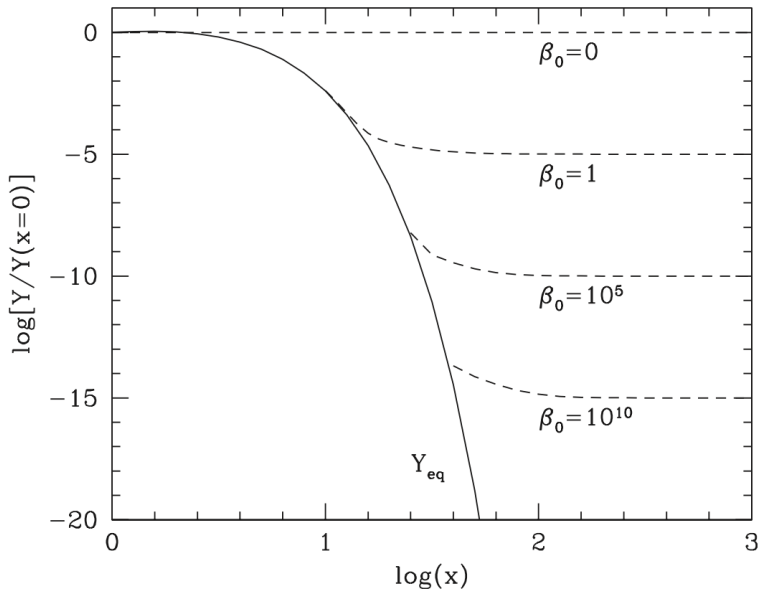

Figure 1.2: The relic abundance for a simple two-body process with a constant $\beta := \langle \sigma v \rangle$.

where we ignored ± 1 in the distribution function $f_{\rm EQ}$ Further ignoring the Pauli block or the Bose enhancement, The second line of the collision term is then greatly simplified as

$$f_X f_{\bar{X}} - f_\psi f_{\bar{\psi}} = e^{-(E_\psi + E_{\bar{\psi}})/T} \left[e^{(\mu_X + \mu_{\bar{X}})/T} - e^{(\mu_\psi + \mu_{\bar{\psi}})/T} \right] = e^{-(E_\psi + E_{\bar{\psi}})/T} \left[\frac{n_X n_{\bar{X}}}{n_X^{\rm EQ} n_{\bar{X}}^{\rm EQ}} - \frac{n_\psi n_{\bar{\psi}}}{n_\psi^{\rm EQ} n_{\bar{\psi}}^{\rm EQ}} \right] , \tag{1.52}$$

where we used the energy conservation $E_\psi + E_{\bar{\psi}} = E_X + E_{\bar{X}}$. Finally, we define the thermally-averaged velocity times cross-section $\langle \sigma v \rangle$ as

$$n_\psi^{\rm EQ} n_{\bar{\psi}}^{\rm EQ} \left\langle \sigma_{\psi\bar{\psi}\to X\bar{X}} |v| \right\rangle := \left(\prod_i \int d^3 p_i \right) (2\pi)^4 \delta^D (p_\psi + p_{\bar{\psi}} - p_X - p_{\bar{X}}) |\mathcal{M}|^2 e^{-(E_\psi + E_{\bar{\psi}})/T} , \tag{1.53}$$

and the Boltzmann equation (1.49) is now

$$\frac{dn_\psi}{dt} + 3Hn_\psi = n_\psi^{\rm EQ} n_{\bar{\psi}}^{\rm EQ} \left\langle \sigma_{\psi\bar{\psi}\leftrightarrow X\bar{X}} |v| \right\rangle \left[\frac{n_X n_{\bar{X}}}{n_X^{\rm EQ} n_{\bar{X}}^{\rm EQ}} - \frac{n_\psi n_{\bar{\psi}}}{n_\psi^{\rm EQ} n_{\bar{\psi}}^{\rm EQ}} \right] . \tag{1.54}$$

With near thermal equilibrium but ψ particles, we arrive at the final expression of the Boltzmann equation

$$\frac{dn_\psi}{dt} + 3Hn_\psi = \langle \sigma v \rangle \left(n_{\psi,{\rm EQ}}^2 - n_\psi^2 \right) . \tag{1.55}$$

At thermal equilibrium, the number density n_ψ will be equivalent to $n_\psi^{\rm EQ}$, and no further net change (creation or annihilation) takes place. If $n_\psi > n_\psi^{\rm EQ}$, more decay of ψ and $\bar{\psi}$ will further reduce n_ψ and increase n_X, and this is reflected in the collision term, where the RHS is negative.

Given the entropy density scales as a^{-3}, it is convenient to define a scaled number density Y that does not change in time as long as $n \propto 1/a^3$,

$$Y_\psi := \frac{n_\psi}{s} , \qquad\qquad Y_\psi^{\rm eq} := \frac{n_\psi^{\rm eq}}{s} . \tag{1.56}$$

The Boltzmann equation is then manipulated in terms of Y as

$$\frac{dY_\psi}{dt} = s \langle \sigma v \rangle \left(Y_{\psi,{\rm eq}}^2 - Y_\psi^2 \right) , \tag{1.57}$$

and by defining a scaled (inverse) temperature x

$$x := \frac{m_\psi}{T} , \qquad t = \frac{1}{2H} \propto \frac{1}{T^2} , \qquad \frac{d\ln t}{dx} = \frac{2}{x} , \tag{1.58}$$

the Boltzmann equation can be written as

$$\frac{x}{Y_\psi^{\rm eq}} \frac{dY_\psi}{dx} = -\frac{n_\psi^{\rm eq} \langle\sigma v\rangle}{H(x)} \left[\left(\frac{Y_\psi}{Y_\psi^{\rm eq}} \right)^2 - 1 \right] . \tag{1.59}$$

The variable x determines if the particle species is relativistic ($x \ll 1$) or non-relativistic ($x \gg 1$), but it also determines the flow of time ($x \gg 1$ at late time). Given the interaction cross-section, the Boltzmann equation can be numerically solved with the initial condition of thermal equilibrium at early time $Y(x=0) = Y_{\rm eq}$ for all species. Assuming a constant cross-section, several solutions to the Boltzmann equation are given in Figure 1.3, in which the equilibrium distribution decays in time as the particle species becomes non-relativistic ($x \simeq 1$) and its abundance is exponentially suppressed compared to the plasma. For a weak cross-section, the particle species decouples early when they are relativistic, and their final abundance is similar to those of photons, rather insensitive of its exact value of the cross-section. For a stronger cross-section, the particles stay in thermal equilibrium longer, and its final relic abundance is sensitively dependent on the value of the cross-section.

A simple analytic approximation can be made to solve the Boltzmann equation. First, the equilibrium abundance $Y^{\rm eq} = n^{\rm eq}/s$ is obtained by using $n^{\rm eq}$ in the relativistic and the non-relativistic cases as

$$Y_\psi^{\rm eq}(x) = \frac{45\zeta(3)}{2\pi^4} \frac{g_\psi^{\rm eff}}{g_{*,s}(x)} \quad \text{for } x \ll 1 , \qquad Y_\psi^{\rm eq}(x) = \frac{90}{(2\pi)^{7/2}} \frac{g_\psi}{g_{*,s}(x)} \, x^{3/2} e^{-x} \quad \text{for } x \gg 1 , \tag{1.60}$$

where $g_\psi^{\rm eff} = g_\psi$ for Boson and $g_\psi^{\rm eff} = 3g_\psi/4$ for Fermion. Clearly, as the Universe evolves (x increases), $Y^{\rm eq}$ also evolves due to the change in $n^{\rm eq}$. Second, the freeze-out (or decoupling) is assumed to be instantaneous, if $\Gamma = H$ at x_f. Equating the interaction rate Γ at equilibrium with the Hubble parameter in RDE

$$H(x) = \frac{8\pi G}{3} \rho_{\rm tot} = \sqrt{\frac{\pi^2 g_*}{90}} \frac{m_\psi^2}{x^2 M_{\rm pl}} , \qquad M_{\rm pl}^2 = \frac{1}{8\pi G} , \qquad \Gamma = Y_\psi^{\rm eq} s \langle\sigma v\rangle , \tag{1.61}$$

we obtain the freeze-out time

$$x_f = \sqrt{\frac{90}{\pi^6 g_*}} \, \zeta(3) g_\psi^{\rm eff} \langle\sigma v\rangle \, m_\psi M_{\rm pl} \quad \text{for } x \ll 1 , \qquad x_f^{-1/2} e^{x_f} = \sqrt{\frac{45}{4\pi^5 g_*}} g_\psi \langle\sigma v\rangle \, m_\psi M_{\rm pl} \quad \text{for } x \gg 1 . \tag{1.62}$$

The condition $x_f \ll 1$ for the relativistic case constrains the strength of $\langle\sigma v\rangle$ and also the mass m_ψ. The freeze-out for the non-relativistic case needs to be solved, but its value is due to the exponential factor highly sensitive to the values in the RHS.

Now we consider the relic densities today. First, they can be relativistic or non-relativistic *today*. The former is similar to the photon distribution, and hence negligible. The latter, non-relativistic relic species today, is often called as the WIMP (weakly interacting massive particles). WIMPS are non-relativistic today, and its energy density is dominated by their rest mass energy. However, it can be relativistic ($x_f \ll 1$) or non-relativistic ($x_f \gg 1$) at the freeze-out. The former is called the hot relic, and their abundance is as much as the photons today, while the latter is called the cold relic.

• ***Relativistic species today***.— The relic density of a relativistic species can then be obtained by using Eq. (1.46) as

$$\frac{\Omega_\psi h^2}{\Omega_\gamma h^2} = \frac{\rho_\psi}{\rho_\gamma} = \frac{g_\psi^{\rm eff}}{2} \left(\frac{T_\psi}{T_\gamma} \right)^4 = \frac{g_\psi^{\rm eff}}{2} \left[\frac{g_{*,s}(x)}{g_{*,s}(x_f)} \right]^{4/3} . \tag{1.63}$$

Given that $g_{*,s}$ always decreases in time and $\Omega_\gamma h^2 = 2.5 \times 10^{-5}$, the relic density of a relativistic species today is as negligible as the photon energy density.

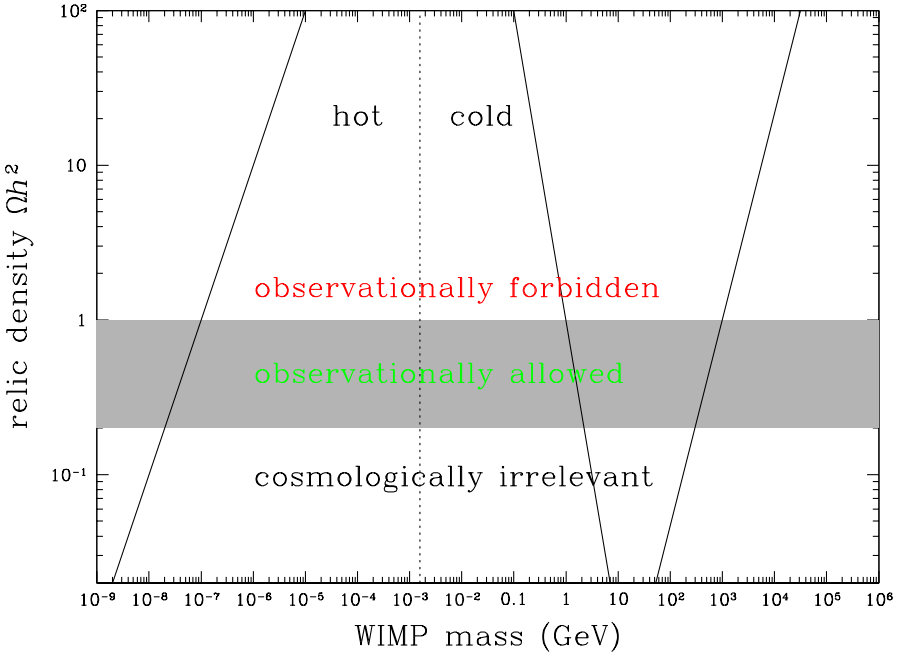

Figure 1.3: Cosmological constraints on the mass of WIMP $\Omega_\psi h^2$.

• ***Hot relics***.— The relic density of a hot species is then

$$\rho_\psi = m_\psi Y_\psi^{\rm eq}(x_f) s(x_0) \quad \propto \quad m_\psi \,, \qquad\qquad \Omega_\psi h^2 = \frac{8\pi G}{3H_0^2}\,\rho_\psi h^2 = 7.64\times 10^{-2}\left[\frac{g_\psi^{\rm eff}}{g_{*,s}(x_f)}\right]\left(\frac{m_\psi}{1\ {\rm eV}}\right) \propto m_\psi \,, \tag{1.64}$$

where x_0 is today. For hot relics, their number density is as large as the photons, and it is rather insensitive to x_f. Note that the dependence of $\langle\sigma v\rangle$ is included in the freeze-out x_f. For a large mass m_ψ, x_f becomes comparable to unity, and it cannot be hot-relic any more. Given the observational constraint $\Omega_{\rm tot}h^2 \lesssim 1$, we can derive that the mass of hot relics should be smaller than

$$m_\psi \le 13.1\ {\rm eV}\left[\frac{g_{*,s}(x_f)}{g_\psi^{\rm eff}}\right] \,, \tag{1.65}$$

which corresponds to

$$m_\nu \le 93.8\ {\rm eV}\,, \qquad\qquad g_{*,s}(x_f) = 10.75\,, \qquad\qquad g_\nu^{\rm eff} = \frac{3}{4}\times 2\times g_\nu \,, \tag{1.66}$$

for massive neutrinos (one species). This cosmological limit is called the Cowsik-McClelland bound. The Planck constraint is $\Sigma m_\nu < 0.23$ eV, and some recent Lyα-forest constraint is < 0.12 eV. The neutrino oscillation constraints give $0.0006 < \omega_\nu < 0.0025$.

• ***Cold relics***.— Similar calculations can be made for cold relics, but the abundance $Y_\psi^{\rm eq}$ is exponentially sensitive to x_f. The LHS for the freeze-out condition

$$x_f^{-1/2} e^{x_f} = \sqrt{\frac{45}{4\pi^5 g_*}}\, g_\psi \,\langle\sigma v\rangle\, m_\psi M_{\rm pl} \,, \tag{1.67}$$

increases monotonically with x_f, i.e., the larger m_ψ or the stronger $\langle\sigma v\rangle$, the later the freeze-out becomes, suppressing the abundance exponentially. Keeping x_f in the equation, we express the abundance and the relic density

$$Y_\psi^{\rm eq}(x_f) = \sqrt{\frac{45}{8\pi^2}}\,\frac{x_f}{\sqrt{g_{*,s}(x_f)}}\,\frac{1}{\langle\sigma v\rangle\, m_\psi M_{\rm pl}} \,, \qquad\qquad \Omega_\psi h^2 = 0.86\frac{x_f}{\sqrt{g_{*,s}(x_f)}}\left[\frac{\langle\sigma v\rangle}{10^{10}\ {\rm GeV}^{-2}}\right]^{-1} \,. \tag{1.68}$$

The relic abundance is sensitively dependent upon $\langle\sigma v\rangle$, and it goes down with m_ψ. While the relic energy density has no explicit dependence on m_ψ, the freeze-out time x_f increases with m_ψ. For example, stable neutrinos of mass between 1 MeV and $m_Z = 100$ GeV fall into this cold relic, and their weak interaction rate is

$$\langle\sigma v\rangle \approx \frac{c_2}{2\pi} G_F^2 m_\nu^2 x^{-b} \qquad \text{for } m_\psi < m_Z \,, \tag{1.69}$$

where $c_2 \simeq 5$ for a Dirac neutrino, $b \sim 1$, and G_F is the Fermi constant. With this, the freeze-out time can be solved as

$$x_f \simeq 17.8 + 3\ln\left(\frac{m_\nu}{1\ \text{GeV}}\right) \,, \tag{1.70}$$

and the relic energy density is

$$\Omega_\nu h^2 \simeq \frac{3.95}{c_2} \frac{x_f^{b+1}}{\sqrt{g_{*,s}(x_f)}} \left(\frac{m_\nu}{1\ \text{GeV}}\right)^{-2} = 1.82 \left(\frac{m_\nu}{1\ \text{GeV}}\right)^{-2} \left[1 + 0.17 \ln\left(\frac{m_\nu}{1\ \text{GeV}}\right)\right] \,, \tag{1.71}$$

The observational constraint puts the mass of stable neutrinos

$$m_\nu \geq 1.4\ \text{GeV} \,, \tag{1.72}$$

and the relic density is smaller with larger mass due to the larger cross-section and the suppression of the abundance. However, for particles of mass $m_\psi \gg m_Z$, the cross-section decreases with particle mass as m^{-2}, instead of increasing with m^2. This implies

$$\Omega_\psi h^2 \simeq \left(\frac{m_\psi}{1\ \text{TeV}}\right)^2 \,, \qquad m_Z \leq m_\psi \leq 3\ \text{TeV} \,. \tag{1.73}$$

For the cold relics, the bound is stronger, because of the non-relativistic freeze-out, and this gives a lower limit for the massive cold relics, called the Lee-Weinberg bound. Figure 1.3 summarizes the cosmological bounds on viable models of WIMPs.

1.3.2 Relic Density of Decaying Particles

If a particle is unstable and decays into other particles, the Boltzmann equation can be supplemented by an extra term for such decay. The number density of decaying particles is always governed by the half-life τ, beyond which the number density is exponentially suppressed as

$$n(t) \propto \exp[-t/\tau] \,, \tag{1.74}$$

but below which the particles behave like stable particles.

If the decay product involves photons, such particles are subject to more stringent observational constraints. A particle decay into photons often involves strong Gamma rays, and these photons should be hidden from observations by preventing the particles decay with longer life-time or by themalizing them. It takes a while to thermalize Gamma ray photons with background radiation, such that the decays must happen early enough.

1.4 Big Bang Nucleosynthesis

Where do we come from? To this philosophical question, here we find some physical answers. The basic structural unit of life is cells that contain lots of molecules, and molecules are electrically neutral groups of atoms held by chemical bonds. Atoms form the smallest unit of the (ordinary) matter, and they are composed of one nucleus and several electrons bound to the nucleus. Where do they come from? Normal stars at the core fuse lighter elements like hydrogen and helium, and more massive stars synthesize carbon, oxygen, and silicon, yielding irons, beyond which no net energy is gained through nuclear fusion. Heavier elements are further generated by neutron captures in supernova explosions. However, observations show that hydrogen and helium are ubiquitous in the Universe with almost constant ratio 75% hydrogen and 24% helium by mass. Indeed, the origin of those elements are primordial and global, rather than localized stars.

1.4.1 Proton and Neutron Abundances

All nuclei are made of protons and neutrons, and they are characterized by its charge number Z (number of protons) and the atomic mass A (number of protons and neutrons). Given their mass $m_p \simeq m_n \simeq 940$ MeV, protons and neutrons are non-relativistic at $t \simeq 10^{-6}$ sec ($T \simeq m_p$) with their number densities

$$n_{n,p} = g_{n,p} \left(\frac{m_{n,p} T}{2\pi}\right)^{3/2} \exp\left[-\frac{m_{n,p} - \mu_{n,p}}{T}\right] , \tag{1.75}$$

and they remain in thermal equilibrium until $T \sim 0.8$ MeV via low-energy weak interactions

$$p + e \leftrightarrow n + \nu_e , \qquad n + \bar{e} \leftrightarrow p + \bar{\nu}_e , \qquad n \leftrightarrow p + e + \bar{\nu}_e . \tag{1.76}$$

Hence the ratio of the number densities in thermal equilibrium is

$$\frac{n_n}{n_p} = \left(\frac{m_n}{m_p}\right)^{3/2} \exp\left[-\frac{m_n - m_p}{T} + \frac{\mu_n - \mu_p}{T}\right] \simeq \exp\left[-\frac{Q}{T}\right] , \qquad Q := m_n - m_p = 1.294 \text{ MeV} , \tag{1.77}$$

where we ignored the difference in the chemical potential $\mu_n - \mu_p = \mu_e - \mu_\nu \simeq 0$ in the weak interactions. At temperature $T \gg Q$, the ratio of the number densities is unity, but it continuously decreases at lower temperature ($T < Q$), because neutrons are slightly heavier than protons. However, due to the neutrino decoupling at $T = 1$ MeV, the weak interactions become inefficient to keep protons and neutrons in thermal equilibrium, such that the ratio freezes out at $T \sim 0.8$ MeV

$$\frac{n_n}{n_p} \sim \exp\left[-\frac{1.294}{0.8}\right] \simeq \frac{1}{5} . \tag{1.78}$$

Free neutrons can further β-decay into protons at any time with its half-life $\tau = 887 \pm 2$ sec ($\simeq 15$ min), which could have exhausted neutrons in our Universe. However, before they decay into protons, most neutrons are indeed captured in deuterium and helium nuclei, where they are stable.[2] By the time the big bang nucleosynthesis is active, the ratio becomes

$$\frac{n_n}{n_p} \simeq \frac{1}{7} \quad \text{at } t \simeq 300 \text{ sec} . \tag{1.79}$$

1.4.2 Nuclear Synthesis of Heavier Elements

With numerous protons and neutrons, they can be forged to form heavier nuclei, but they are dissociated immediately by energetic photons, until the Universe cools below their binding energy (e.g., 2.22 MeV for deuterium). In thermal equilibrium, the abundance of nuclei with atomic mass A with charge Z is

$$n_A = g_A \left(\frac{m_A T}{2\pi}\right)^{3/2} \exp\left[-\frac{m_A - \mu_A}{T}\right] = g_A \left(\frac{m_A T}{2\pi}\right)^{3/2} \exp\left[-\frac{m_A}{T}\right] \left[\exp\left(\frac{\mu_p}{T}\right)\right]^Z \left[\exp\left(\frac{\mu_n}{T}\right)\right]^{(A-Z)} , \tag{1.80}$$

where we used the relation for the chemical potential

$$\mu_A = Z\mu_p + (A - Z)\mu_n . \tag{1.81}$$

With the same formulas for the proton and the neutron number densities in equilibrium, we can remove the chemical potentials μ_p and μ_n in favor of n_p and n_p to express

$$n_A = \frac{g_A A^{3/2}}{g_N^A} n_p^Z n_n^{A-Z} \left(\frac{m_N T}{2\pi}\right)^{\frac{3}{2}(1-A)} \exp\left(\frac{B_A}{T}\right) , \qquad g_N := g_p = g_n = 2 , \tag{1.82}$$

[2] Sometimes, Pauli's exclusion principle is invoked for such stability, but neutrons do decay in nuclei, when energetically favorable. In nuclei, all the neutrons and protons form a system, in which protons typically occupy higher energy state due to electromagnetic repulsion, such that nuclei with somewhat more neutrons than protons are stable, because converting one neutron into a proton would need more energy. Of course, if even more neutrons are present in nuclei, they inevitably occupy higher energy state than protons, and β-decay is then energetically favorable.

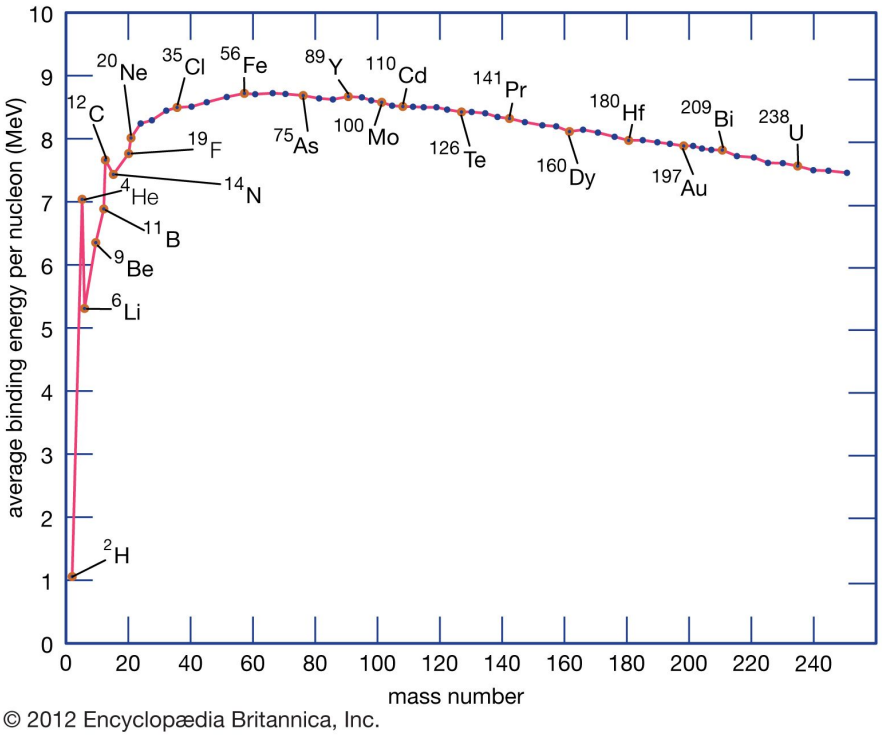

Figure 1.4: Average binding energy of nuclei per proton. With the steep increase in the binding energy, nuclear fusion is an efficient way to generate energy up to iron, beyond which the binding energy decreases. Nuclear fission can be used for elements heavier than irons to extract energy, though not as efficient as nuclear fusion.

where we approximated $m_N := m_p \simeq m_n$ and $m_A \simeq A m_N$, and defined the binding energy of nucleus

$$B_A := Z m_p + (A - Z) m_n - m_A \,. \tag{1.83}$$

In the presence of heavier elements, the baryon number density is

$$n_b := n_p + n_n + \sum_i A_i n_{A,i} \,, \tag{1.84}$$

and the mass fraction of each nucleus A:

$$X_{A_i} := \frac{A_i n_{A,i}}{n_b} \,, \qquad 1 = \sum_i X_{A,i} \,. \tag{1.85}$$

The baryon number density includes free neutrons and protons, but also accounts for those inside nuclei with weight A_i, i.e., it is the total number densities of protons or neutrons, while the mass fraction shows how many nuclei are captured in the nucleus. The number density of nucleus A can then be re-expressed by using n_γ in Eq. (1.20) as

$$X_A = \frac{g_A}{2} A^{5/2} \left[\frac{4\zeta(3)}{\sqrt{2\pi}}\right]^{A-1} X_p^Z X_n^{A-Z} \eta^{A-1} \left(\frac{m_N}{T}\right)^{\frac{3}{2}(1-A)} \exp\left(\frac{B_A}{T}\right) \,, \tag{1.86}$$

where we defined the baryon-to-photon ratio:

$$\eta := \frac{n_b}{n_\gamma} = 2.72 \times 10^{-8} \omega_b \left(\frac{T_{\rm cmb}}{2.73\,{\rm K}}\right)^{-3} \approx 5 \times 10^{-10} \,. \tag{1.87}$$

As the temperature of the Universe cools below the binding energy, nuclei with atomic mass A can form, and for the mass fraction to be non-negligible ($X_A \simeq 1$), the temperature has to be below

$$\ln X_A \simeq 0 \,, \qquad T_A \approx \frac{|B_A|}{(A-1)\left[|\ln \eta| + \frac{3}{2}\ln(m_N/T_A)\right]} \,. \tag{1.88}$$

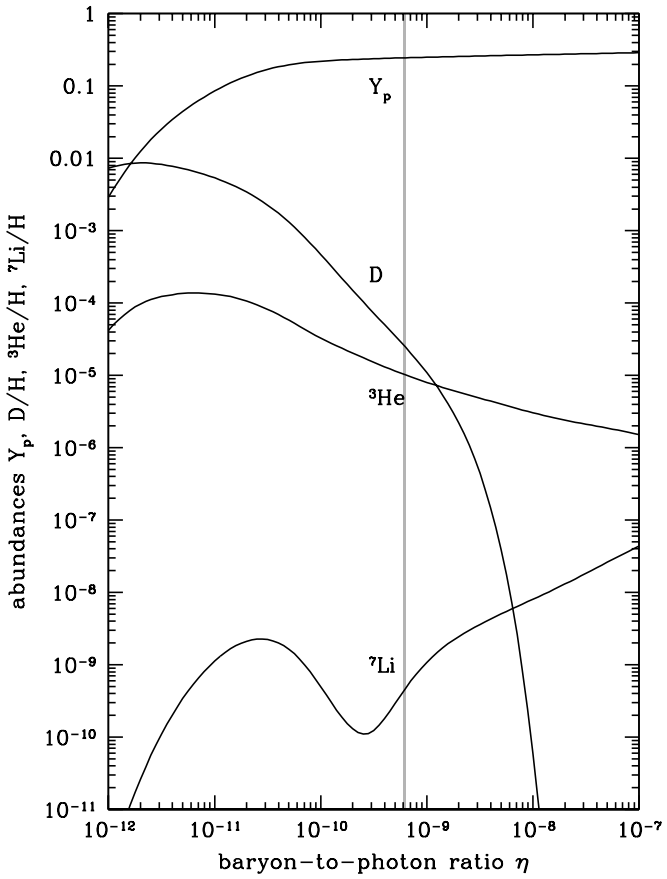

Figure 1.5: Primordial abundances of light elements as a function of the baryon-to-photon ratio.

The deuterium ^{2}D has the lowest binding energy $B_D = 2.22$ MeV, but the formation of deuterium takes place only when the temperature of the Universe is an order-of-magnitude below $B_D \simeq 2 \times 10^{10}$ K due to large number of photons. The high-energy tail (Wien) of the photon distribution is sufficiently large enough to destroy deuterium nuclei, until it reaches $T_D \approx 10^9$ K ($t \sim 100$ sec). This is the beginning of the Big Bang Nucleosynthesis (BBN).

Once the nucleosynthesis begins, many channels of nuclear reaction take place. However, since the number densities of nuclei in the Universe are quite low at the time of BBN, only two-body interactions are possible, and the fact that there are no stable nuclei with atomic mass 5 or 8 implies that no elements heavier than lithium ^{7}Li (3 protons) can be produced. The next element in periodic table is ^{9}Be (4 protons). In contrast, at the core of massive stars, where the densities are even higher, many-body interaction channels are allowed, and even a short-lived ^{8}Be that formed through ^{4}He-^{4}He collision can quickly capture another ^{4}He to form a stable carbon ^{12}C, allowing further nuclear reactions to proceed.

Since the binding energy of deuterium is the lowest, the formation of deuterium nuclei acts as a bottleneck for nucleosynthesis, as heavier elements are already allowed to form by T_D. Consequently, almost all the deuterium nuclei (or free neutrons) are processed to form helium nuclei, and the mass fraction of helium is

$$Y := X_{^4\mathrm{He}} \simeq \frac{4(n_n/2)}{n_n + n_p} = \frac{2(n_n/n_p)_D}{1 + (n_n/n_p)_D} \approx \frac{1}{4}\,, \qquad \left(\frac{n_n}{n_p}\right)_D \approx \frac{1}{7}\,, \tag{1.89}$$

where the subscript D indicates the time of deuterium formation, when helium nuclei are yet to form, i.e., $n_b = n_n + n_p$. Observations of the helium mass fraction is about 24% everywhere, and the confirmation of this prediction for He is one of the success of the Big Bang model in the early days.

The predictions of primordial nucleosynthesis and their observational confirmation is of course important. In particular, it helps constrain η or the baryon density ω_b. However, it is in fact not easy to determine the primordial abundances from observations, because the observed abundances have been re-processed through stars and other astrophysical events. In the following we give a brief summary of the present observational situation (Mo et al., 2010):

- ^{4}He: With its large abundances, it is relatively easy to make observations, and the abundances are often estimated from ionized HII clouds by using the recombination lines. Since ^{4}He can be produced in stars, the estimates are the upper bound of the primordial abundances. In order to reduce this contamination, observers often target metal-poor gas clouds. In reality, observations are made as a function of metalicity, and the helium abundance is estimated by extrapolating it to zero-metalicity. The current estimate is $Y_p = 0.24 \pm 0.01$, but its abundance is relatively insensitive to η.

- ^{2}D: The deuterium abundance is estimated from UV absorption lines in the interstellar medium or in Lyα clouds at high redshifts. Since deuterium is rather weakly bound, it is easy to destroy them, but at the same time, it is hard to produce in stars. Therefore, the deuterium estimates serve as a lower bound. In particular, Lyα clouds at high redshifts are quite close to primordial. The local estimates give [D/H]$\simeq 1.6 \times 10^{-5}$, while the estimates from Lyα clouds yield $2.82 \pm 0.53 \times 10^{-5}$. Since the deuterium abundance sensitively changes with ω_b, its measurements are crucial in determining ω_b.

- ^{3}He: The abundance of ^{3}He can be measured by using meteorites and the solar wind in the solar system or by measuring the strength of the ^{3}He+ hyperfine transition line in HII regions. Old meteorites should contain material at the formation of the solar system. Since ^{2}D can be burned to ^{3}He in the Sun, the sum of (D+^{3}He) is a good measure of the pre-solar abundance from the solar wind. While ^{3}He can be destroyed at the core of stars, it is much harder than ^{2}D. The current measurements from the Solar system give an upper limit on $[(\mathrm{D} + {}^3\mathrm{He})/\mathrm{H}] < 10^{-4}$.

- ^{7}Li: Estimates of the ^{7}Li abundance come from stellar atmospheres. Since ^{7}Li is quite fragile, they are depleted if transported deeper into the centers of stars, which results in significant variations in observations. With weak convection, the estimates from metal-poor stars are believed to be more robust and close to the primordial abundances. The current observations yield $[^7\mathrm{Li}/\mathrm{H}] \simeq (1.5 \pm 0.4) \times 10^{-10}$.

With precise determination of T_γ and ω_b from CMB measurements, the predictions of BBN are completely fixed under the standard model of particle physics and cosmology, and they are used for consistency check with observations, in particular, of the abundances of ^{4}He and ^{2}D. On the other hand, the situation with ^{3}He is too complex for a meaningful comparison to be possible, and the results for ^{7}Li appear to disagree within uncertainties. This discrepancy reflects observational challenges in inferring the primordial abundances, but it might imply that the early Universe might have been different from what the standard model physics predicts.

1.5 Recombination and Matter-Radiation Decoupling

1.5.1 Recombination of Hydrogen Atoms

Once the nucleosynthesis is completed, the Universe consists of protons, helium nuclei, electrons, photons, decoupled neutrinos, and a trace amount of other elements such as ^{2}D, ^{3}He and so on. All particles except photons and neutrinos are already non-relativistic, and they stay in thermal equilibrium mainly through the electromagnetic interactions. As the Universe cools, the next cosmological event is to form neutral hydrogen atoms by combining free electrons and protons, which is called the cosmic recombination.

Assuming the thermal equilibrium and $\mu_H = \mu_p + \mu_e$, we can derive the hydrogen number density in the exactly same way to Eq. (1.82) as

$$n_H = \left(\frac{g_H}{g_p g_e}\right) n_p n_e \left(\frac{m_e T}{2\pi}\right)^{-3/2} \exp\left(\frac{B_H}{T}\right) , \qquad g_H = g_e = 2 , \quad g_p = 1 , \tag{1.90}$$

where the binding energy of hydrogen atoms is

$$B_H := m_p + m_e - m_H = 13.6 \text{ eV} . \tag{1.91}$$

Mind that the degeneracy factor for electrons in neutral hydrogen atoms is $g_H = \sum 2n^2 \simeq 2$ and that for ionized protons is $g_p = 1$. Ignoring helium or any other elements $n_b \simeq n_p + n_H$ and assuming $n_e = n_p$, the hydrogen number density can be re-expressed as

$$\frac{n_H}{n_b} = \left(\frac{n_e}{n_b}\right)^2 \eta \, n_\gamma \left(\frac{m_e T}{2\pi}\right)^{-3/2} \exp\left(\frac{B_H}{T}\right) . \tag{1.92}$$

By defining the ionization fraction (or how many free electrons), we arrive at the Saha equation for the ionization fraction in thermal equilibrium:

$$X_e := \frac{n_e}{n_b} = \frac{n_p}{n_b} \le 1 , \qquad \frac{1 - X_e}{X_e^2} = \sqrt{\frac{32}{\pi}} \zeta(3) \, \eta \left(\frac{m_e}{T}\right)^{-3/2} \exp\left(\frac{B_H}{T}\right) . \tag{1.93}$$

Once the Universe cools below the binding energy B_H, the hydrogen atoms can form, but again due to the large number of high-energy photons at a given temperature compared to baryons, the formation of neutral hydrogen atoms is further delayed. If we define the completion of the recombination process as $X_e = 10\%$, the Saha equation states

$$\theta_{\rm rec}^{-3/2} \exp\left(\frac{13.6}{\theta_{\rm rec}}\right) = \frac{0.9}{0.01} \left(\sqrt{\frac{32}{\pi}} \zeta(3) \, \eta\right)^{-1} \left(\frac{m_e}{1 \text{ eV}}\right)^{3/2} = 3.2 \times 10^{17} \, (\omega_b)^{-1} , \tag{1.94}$$

where we defined

$$\theta := \frac{T}{1 \text{ eV}} \simeq \frac{1+z}{4250} . \tag{1.95}$$

A numerical computation yields that the recombination takes place at

$$1 + z_{\rm rec} \approx \frac{1367}{1 - 0.024 \ln \omega_b} \approx 1249 , \qquad T_{\rm rec} = 0.3 \text{ eV} \ll B_H , \tag{1.96}$$

a lot lower temperature than B_H.

There are a few subtleties in the cosmic recombination. In a typical gas cloud, the recombination process takes place by a direct capture of free electrons to the ground state (case A recombination) or cascades of electronic transition to the ground state (case B recombination). Both of which are inefficient in the cosmic recombination, because both processes result in high energy photons that ionize hydrogen atoms again. The main channel in the cosmic recombination is a forbidden transition with $\Gamma \approx 8.23$ sec^{-1}, so called, the two-photon decay, in which two photons are emitted by an electronic transition $2s \to 1s$, splitting the energy of Lyα. The other process is the cosmological redshift of Lyα photons. The detailed numerical computation shows that the ionization fraction $X_e = 1$ at $z \ge 2000$ decreases as the Universe cools, and it freezes out to a value $X_e \simeq 10^{-3}$ at $z \le 200$.

1.5.2 Decoupling of CMB Photons and Baryons

• ***Decoupling of CMB photons***.— The baryon-photon plasma (including leptons) maintains the equilibrium via Coulomb interactions between photons and free electrons. At this low energy scales, the interaction is mainly elastic, and its cross-section is described by the Thompson scattering as

$$\sigma_T := \frac{8\pi}{3} r_e^2 \simeq 6.651 \times 10^{-25}\ \mathrm{cm}^2\ , \qquad r_e := \frac{e^2}{m_e c^2} = 2.818 \times 10^{-13}\ \mathrm{cm}\ , \tag{1.97}$$

where the radius of an electron is defined in terms of the Coulomb potential. The Thompson scattering describes a classical collision of ionized electrons. With higher mass, the Thompson scattering cross section for protons is smaller by $(m_e/m_p)^2 = 10^6$ and negligible, but the strong Coulomb interactions between free electrons and protons also keep the protons in thermal equilibrium. As the Universe cools and free electrons recombine to form neutral hydrogen atoms, the interaction rate in the baryon-photon plasma goes down:

$$n_e = X_e\, \eta\, n_\gamma\ , \qquad \Gamma_\gamma = n_e \sigma_T c = 1.01 \sqrt{\omega_b}\, \theta^{9/4} \exp\left[-\frac{6.8}{\theta}\right]\ \mathrm{sec}^{-1}\ , \tag{1.98}$$

and the photons are released (or decoupled) from the plasma, when the interaction rate becomes lower than the expansion rate:

$$H \simeq H_0 \sqrt{\Omega_m} (1+z)^{3/2} = 8.98 \times 10^{-13} \sqrt{\omega_m}\, \theta^{3/2}\ \mathrm{sec}^{-1}\ , \tag{1.99}$$

where we assumed that the Universe is deep in the matter dominated era. The decoupling takes place at

$$\theta_{\rm dec}^{-1} \approx 3.927 + 0.074\ \ln\left(\frac{\omega_b}{\omega_m}\right)\ , \qquad T_{\rm dec} = 0.26\ \mathrm{eV}\ , \qquad 1 + z_{\rm dec} \simeq 1100\ , \tag{1.100}$$

soon after the recombination of neutral hydrogen atoms takes place. Another way of understanding the decoupling of photons is to compute the optical depth:

$$\tau(z) := \int_0^z dz\, \frac{c\, dt}{dz} n_e \sigma_T \approx 0.37 \left(\frac{z}{1000}\right)^{14.25}\ , \tag{1.101}$$

where the numerical values are approximations to the best-fit model prediction. The Universe is fairly transparent at low redshift, and it becomes quickly opaque around $z_{\rm dec}$. A simple analytic calculation shows that the observed CMB photons are indeed emitted at the peak of the visibility function defined as

$$P(\tau) := \tau e^{-\tau(z)}\ . \tag{1.102}$$

which peaks sharply at $z \simeq 1067$ with a width $\Delta z \simeq 80$. In other words, before the decoupling, the CMB photons were in thermal equilibrium with baryons via Thompson scattering, and they are un-polarized and opaque. However, within a narrow redshift width, they are released from the baryon plasma, and they are weakly polarized via last scattering.

• ***Decoupling of baryons***.— Now we consider the decoupling of baryons from the baryon-photon plasma. While the photons are released at $z_{\rm dec} \simeq 1100$, the baryons are kept in thermal equilibrium long after the decoupling of photons, due to large number of photons per baryons. In general, the matter components cool as $T_m \propto 1/a^2$, faster than the photons, but because of the tight coupling it goes as $T_m \sim T_\gamma \propto 1/a$ until it is released from the photon plasma, i.e., energy is transferred to the baryon plasma from the photon plasma by the Compton scattering of high-energy photons. For the decoupling of photons, the relevant interaction rate was Γ_γ, and no energy transfer was made. For the decoupling of baryons, however, we have to account for this energy transfer to compute the proper interaction rate Γ_e.

The typical average energy transfer due to one Compton scattering of high-energy photons is given by

$$\Delta E = \frac{4}{3}\left(\frac{v_e}{c}\right)^2 \bar{E}_\gamma = 4\left(\frac{kT_e}{m_e c^2}\right)\frac{u_\gamma}{n_\gamma}\ , \qquad \bar{E}_\gamma = h\bar{\nu} = \frac{u_\gamma}{n_\gamma}\ , \tag{1.103}$$

and with larger number of photons n_γ, the energy transfer rate per unit volume is then

$$\frac{d\epsilon}{dt} = \Delta E\ n_\gamma \Gamma_\gamma = 4 n_e \sigma_T u_\gamma \left(\frac{kT_e}{m_e c}\right)\ . \tag{1.104}$$

Since free electrons are tightly coupled with free protons, this energy transfer is quickly shared with protons of typical energy density

$$\epsilon_m = \frac{3}{2}(n_e + n_b)kT_e \ . \tag{1.105}$$

Therefore, the proper interaction rate for electrons to be compared to the expansion rate is then

$$\Gamma_e = \frac{1}{\epsilon_m}\frac{d\epsilon}{dt} = 8.9 \times 10^{-6}\left(\frac{X_e}{1+X_e}\right)\theta^4 \ \mathrm{sec}^{-1} \ , \tag{1.106}$$

and the baryon plasma decouples at

$$1 + z = 6.8\left(\frac{X_e}{1+X_e}\right)^{-\frac{2}{5}} \omega_m^{1/5} \approx 150 \ . \tag{1.107}$$

Note that the Compton scattering conserves the number of photons, such that it can lead to a spectral distortion. However, the small baryon-to-photon ratio makes it negligible for the photon plasma. The free-free emission and absorption (Bremsstrahlung) can create and destroy photons, such that it is needed to thermalize. However, this process is inefficient at $T \leq 10^4$ eV.